Hindawi
Shock and Vibration
Volume 2021, Article ID 6643773, 12 pages
https://doi.org/10.1155/2021/6643773

Research Article

Effect of Concentration and Suspension Agent (HPMC) on Properties of Coal Gangue and Fly Ash Cemented Filling Material

Baogui Yang,[1,2] Junyu Jin,[1,2] Xindong Yin,[3] Xiaoyu Wang,[1] and Hongliang Yang[3]

[1]*School of Energy and Mining Engineering, China University of Mining & Technology-Beijing, D11 Xueyuan Road, Haidian District, Beijing 100083, China*
[2]*State Key Laboratory of Coal Resources and Safe Mining, China University of Mining and Technology-Beijing, D11 Xueyuan Road Haidian District, Beijing 100083, China*
[3]*Chifeng Chaihulanzi Gold Mining Co., Ltd., Chaihulanzi Village, Chutoulang Town, Songshan District, Inner Mongolia Autonomous Region, Chifeng City 024039, China*

Correspondence should be addressed to Junyu Jin; junyu.jin@student.cumtb.edu.cn

Received 21 December 2020; Revised 7 January 2021; Accepted 25 January 2021; Published 8 February 2021

Academic Editor: Guangchao Zhang

Cemented coal gangue-fly ash backfill (CGFB) mixtures are utilized as the filling materials for backfilling the underground openings in coal mines. The freshly prepared CGFB slurries are commonly transported into the gobs through a pipeline. The mixture ratio of slurry concentration and suspending agent (HPMC) plays an essential role in transporting the slurry to goaf smoothly and efficiently. In this paper, the influence of slurry concentration and HPMC on the performance of coal gangue-fly ash cemented filling material was studied based on the response surface method. The prediction model of CGFB slurry slump flow, segregation rate, and bleeding rate was constructed. It is concluded that the segregation rate and slump flow of slurry are more sensitive to the variation of concentration. On the other hand, the bleeding rate of slurry is more sensitive to the change of HPMC content. Based on the established model, the reasonable mix proportion range of slurry concentration and suspending agent (HPMC) was obtained. In addition, three new CGFB mixtures have been tested, and the experimental results are in good agreement with the predicted values.

1. Introduction

While coal has made great contributions to China's economic development and social construction, it also inevitably causes some problems, mainly including the destruction and occupation of land resources, the destruction and pollution of water resources, and the destruction and pollution of atmospheric environment. The destruction and occupation of land resources are mainly caused by surface subsidence and gangue piling caused by underground mining [1]. The damage and pollution of water resources is manifested in the natural drainage of aquifer caused by water flowing fissures in the mining process, which damages the groundwater resources and even leads to river cutoff and river drying up. The destruction and pollution of atmospheric environment mainly refers to the pollution caused by spontaneous combustion of gas and gangue discharged into the air with mining. In addition, the fine solid particles in the gangue hill will form dust with the wind and pollute the environment [2].

Cemented filling mining is one of the most popular techniques in the green mining technology system in coal mine. It takes broken coal gangue as aggregate and ordinary Portland cement and fly ash as cementation material with the addition of admixture (HPMC) and water to form high-concentration slurry in a certain proportion. Cemented filling of goaf can effectively reduce the subsidence of coal seam roof, the pressure of mining face, and the change of strata. It also protects water resources, prevents environmental problems, and reduces the ground gangue [3–5]. It is an effective way to solve the environmental problems of coal mining and the "three under" coal mining problems [6–9].

Scholars at home and abroad have done some research on the cemented coal gangue-fly ash backfill (CGFB). Wu et al. [10] determined the flow properties of the CGFB slurry based on the Looping pipe experiments and developed a pipe flow model for predicting the flow behavior of the CGFB slurry in the pipe loop. Yin et al. [11] proposed an electrochemical treatment to improve the early age strength and deformation characteristics of CGFB. Hou et al. [12] studied the mechanical properties of CGFB with cracks under different seepage water pressures, introducing the damage variable which can evaluate the seepage effect and crack effect, and discussed the damage evolution law of CGFB with cracks under the seepage-stress coupling, which is based on the theory of damage mechanics. Li et al. [13] studied the effect of material composition on the performance of superplasticizer when the target slump was 250 mm by response surface methodology. Wang [14] studied the proportion of cemented coal gangue-fly ash backfill mixtures, considering that when the mass ratio of cement fly ash to coal gangue is 1 5 :4 : and the mass fraction of solid material reaches 72% ~ 75%, the quality indexes of cement slurry such as strength, dehydration rate, and pipeline characteristics can meet the requirements of goaf backfilling. Wu et al. [15] carried out an experimental study on the transportability and pressure drop of the CGFB slurry through the loop pipe with the help of a pipe loop system built in laboratory and revealed and discussed the effects of solids concentration as well as ratios of coal gangue to fly ash, fly ash to Portland cement, and coal gangue to Portland cement on the pressure drop of the loop pipe flow of the fresh CGFB slurry samples [11–14, 16–22].

Although domestic and foreign scholars have done some research on CGFB mixtures, there is little research on the effect of HPMC and concentration on the performance of CGFB slurry. Fresh CGFB slurry is transported to the goaf for filling through a pipeline with an inner diameter of 150–180 mm and a length of about 2000 m [23, 24]. Pipe blockage often occurs in the actual field transportation process. The main reasons for pipe blockage are as follows: (1) high slurry concentration leads to large pipeline transportation resistance, and the required pump pressure exceeds the limit of working pressure of the pump, resulting in pipe blockage. (2) In order to ensure the fluidity of the slurry, the concentration of the slurry is reduced, resulting in the separation of coarse aggregate (gangue particles) and fine-grained (fly ash and cement) in the process of transportation. The gangue particles settle to the bottom of the pipeline, which results in pipe blockage. Changing the slurry concentration alone cannot solve the problem of pipe plugging. In order to address this problem, the method is to control the slurry concentration in the appropriate range and to add an appropriate amount of HPMC into the slurry, which will make the slurry have less transport resistance and ensure the appropriate segregation rate. Pipe plugging is expected to be avoided and CGFB slurry will be transported to the goaf smoothly.

This paper aims to study the influence of slurry concentration and HPMC on slurry performance and obtain an optimum mix ratio of slurry concentration and HPMC. Response surface methodology (RSM) is to use the appropriate test design method to design the test scheme and then run the test according to the order of the test scheme to obtain certain test data; use multiple regression equation to fit the quantitative relationship between test factors and response variables. Finally, the regression equation analysis is used to find the optimal response level. Response surface method is a method to solve the multivariable problem of mathematical statistics. Response surface method includes many experimental design and data processing techniques, such as experimental design, regression equation modeling, model significance test, and factor combination condition optimization. By fitting the functional relationship between the response and various factors, drawing the response surface and contour line, the response value corresponding to each factor level can be easily obtained; then the optimal response value corresponding to the level of each factor can be found out [25–28].The RSM has several advantages, such as the efficiency to predict the model for each response, to construct a robust model with a small number of experimental data points, to assess the interaction effect between the factors, and to locate the optimal response [29–31].

2. Materials and Methods

2.1. Materials. In the present study, the materials used are coal gangue from "Linxi" mine and fly ash from nearby power plant, ordinary Portland cement, and water conforming to ASTM C150. The density of coal gangue is 2300 kg/m^3. The particle size distribution of coal gangue, fly ash, and cement used in this study is shown in Figure 1. The chemical composition of coal gangue, fly ash, and cement is shown in Table 1.

2.2. Experimental Design Method. The first step of response surface methodology (RSM) is to carry out experimental design. There are many kinds of RSM design methods, including Box–Behnken design and central composite design (CCD), optimal design, Bayesian design, and robust design. In this paper, optimal design based on RSM was conducted by using Design-Expert 8.0.5 software. In the optimal design, the slurry concentration and dosage of HPMC are taken as independent variables. Table 2 indicates variable levels in the form of actual and coded values, the slurry concentration varies from 77% to 80%, and the HPMC dosage is from 0% to 1.5%. The segregation rate, bleeding rate, and slump flow of slurry are taken as dependent variables. The functional relationship between selected independent and dependent variables can be expressed as

$$Y = f\left(X_1, X_2, X_3, \ldots\ldots, X_N\right) + \varepsilon, \tag{1}$$

where Y signifies the dependent variable, $X_1, X_2, X_3, \ldots, X_n$ denote the independent variables, f represents the dependent variable function, and ε implies the experimental error.

For optimal design, the matrix form of dependent variable is written as follows:

$$Y = X\alpha + \varepsilon, \tag{2}$$

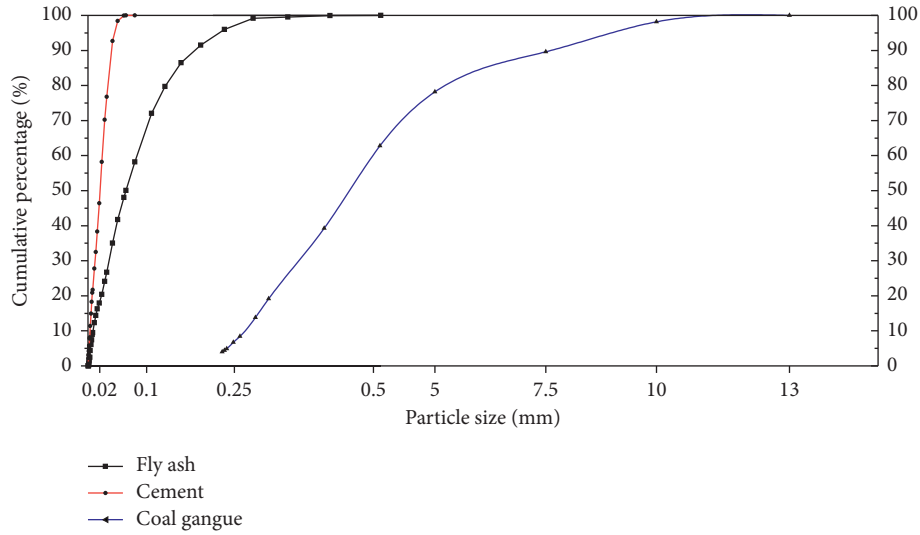

Figure 1: Distribution of material particles' size.

Table 1: Chemical composition of materials.

Chemical component	Cement	Fly ash	Coal gangue
SiO_2	19.68	53.85	43.77
Al_2O_3	4.57	32.88	21.52
CaO	62.59	1.64	22.64
Fe_2O_3	3.53	5.59	5.27
S	2.56	0.72	3.4
TiO_2	—	1.97	1.32
MgO	3.17	—	—

Table 2: The actual and coded values of the experimental factors.

Concentration (%)	Suspending agent (‰)	Coded values
77	0	−1
78.5	0.75	0
80	1.5	1

where X denotes the matrix of model terms, α implies the vector of regression coefficients, and α can be determined with the least-squares technique. It is shown as follows:

$$\alpha = \left(X^T X\right)^{-1} X^T Y, \tag{3}$$

where X^T indicates the transpose of the matrix X.

In optimal design algorithm, from all possible design points, the experimental design points which maximize the determinant of |XTX| are determined by means of a computer program [32].

2.3. Mixture Proportions. In this paper, on the basis of a large number of previous experiments, the proportion of coal gangue and fly ash cemented filling material is determined. When the cement content is 12% of the total weight and the weight ratio of fly ash to gangue is fixed at 0.4, the material can maintain a good gradation, and the 28 d strength of the material can reach 4 MP, which can meet the strength requirements. The ranges of concentration and HPMC are given in Table 2. The optimal design method under response surface in Design-Expert 8.0.5 software is used to design the experiment. The experimental design scheme is shown in Table 3.

2.4. Testing and Evaluation Methodology

2.4.1. Fluidity Test. A trumpet-shaped slump bucket with an upper diameter of 100 mm, a lower diameter of 200 mm, and a height of 300 mm was placed on the specified position of the slump flow plate according to the regulations, and the fresh slurry was filled in three times. After each filling, the tamping hammer shall be used to evenly strike 25 times along the barrel wall from the outside to the inside; then the CGFB slurry was smoothed. Then, pull out the bucket and use the average diameter of slurry after flow, namely, slump flow, as the liquidity index to measure the fluidity of fresh CGFB slurry. The measuring equipment is shown in Figure 2.

2.4.2. Segregation Rate Test. The segregation rate of fresh slurry is tested by the device shown in Figure 3(a). The device consists of four cylindrical plastic pipes with a diameter of 80 mm and a height of 80 mm. The fresh slurry is poured into the test device and left standing for 2 hours. After that, the slurry in each section of pipe is taken out and washed with water. The gangue particles with particle size greater than 5 mm in each section are selected and weighed and counted, respectively. Figure 3(b) shows the gangue with particle size larger than 5 mm screened out by washing in each section. According to formula (4), the segregation rate of slurry with different proportions is calculated.

$$S = \sum_{i=1}^{i=3} \frac{2\left(W_{i+1} - W_i\right)}{3\left(W_{i+1} + W_i\right)}, \tag{4}$$

where S is the segregation rate, %, and W is the weight of gangue with particle size greater than 5 mm in each pipe section, g.

Table 3: Experimental design scheme.

Samples	Solids content (wt. %)	Cement content (wt. %)	Fly ash content (wt. %)	Coal gangue content (wt. %)	HPMC content/powder (wt. %)	Water content (wt. %)
1#	77.00	12.00	18.57	46.43	0.49	23.00
2#	77.00	12.00	18.57	46.43	0.49	23.00
3#	77.00	12.00	18.57	46.43	1.50	23.00
4#	77.00	12.00	18.57	46.43	1.50	23.00
5#	77.57	12.00	18.73	46.84	1.00	22.43
6#	77.84	12.00	18.81	47.03	0.00	22.16
7#	77.84	12.00	18.81	47.03	0.00	22.16
8#	78.43	12.00	18.98	47.45	1.50	21.57
9#	78.68	12.00	19.05	47.63	0.86	21.32
10#	78.88	12.00	19.11	47.77	0.28	21.12
11#	79.69	12.00	19.34	48.35	1.01	20.31
12#	79.97	12.00	19.42	48.55	0.51	20.03
13#	80.00	12.00	19.43	48.57	0.00	20.00
14#	80.00	12.00	19.43	48.57	0.00	20.00
15#	80.00	12.00	19.43	48.57	1.50	20.00
16#	80.00	12.00	19.43	48.57	1.50	20.00

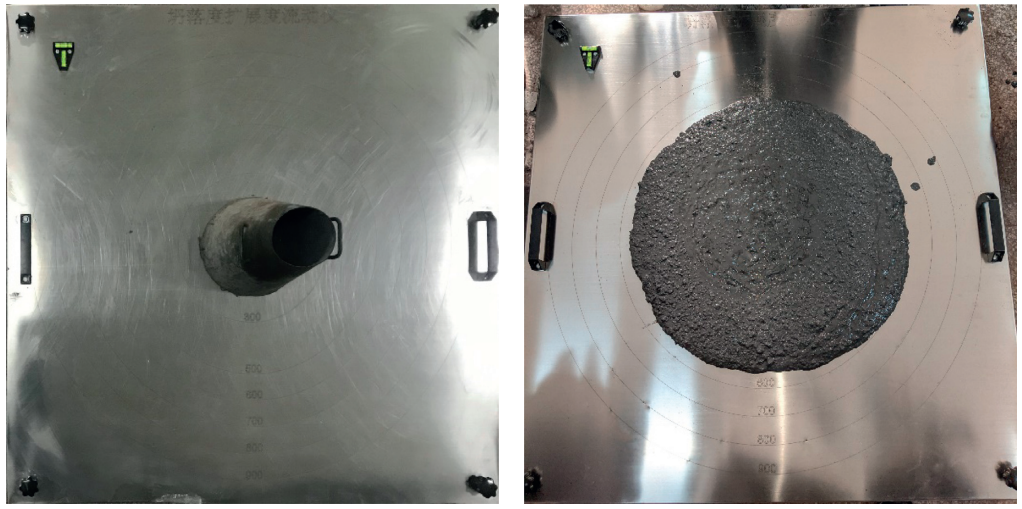

(a) (b)

Figure 2: Graph of slump flow test. (a) Measuring device. (b) Slump flow measurement.

2.4.3. Bleeding Rate Test. The bleeding rate of slurry was tested with a 5 L (inner diameter of 185 mm and height of 200 mm) cylinder with cover as shown in Figure 4. Firstly, wet the cylinder with wet cloth, put the CGFB mixture into one time, vibrate on the vibration table for 20 s, and then gently smooth it with a spatula and cover it to prevent water and evaporation. The surface of the sample should be about 20 mm lower than the edge of the cylinder. Start to calculate the time after plastering. In the first 60 minutes, suck out the bleeding with a pipette every 10 minutes; then suck water every 20 minutes until there is no bleeding for three consecutive times. 5 minutes before each water absorption, the bottom side of the cylinder should be padded up by about 20 mm to make the cylinder inclined to facilitate water absorption. After absorbing water, put the cylinder gently flat and cover. The total bleeding volume is calculated with an accuracy of 1 g. The bleeding rate is calculated according to formula (5).

$$B = \frac{V_W}{(W/G)(G_1 - G_0)} \times 100, \tag{5}$$

where B is the bleeding rate, %; V_W is the total mass of bleeding, g; W is the water consumption of CGFB mixture; G is the total mass of CGFB mixture, g; G_1 is the mass of cylinder and sample, g; and G_0 is the mass of cylinder, g.

3. Results and Discussion

3.1. Model Fitting and Analysis. The measured results of the factors for 16 mixtures in Table 4 were used to derive the

(a) (b)

Figure 3: Graph of segregation rate test. (a) Measuring device. (b) Gangue particles with particle size greater than 5 mm.

(a) (b)

Figure 4: Graph of bleeding rate test. (a) Measuring device. (b) Bleeding rate measurement.

regression models. All the coefficients of the models (equation (1)) were determined by the least-squares approach, using Design-Expert 8.0.5. In the process of establishing the model, after collecting the experimental data, the data is input into Design-Expert 8.0.5. The software will analyze the data and recommend the fitting model according to the characteristics of the data. The model recommended by the software is used for fitting, and the fitting results are tested. The importance of each model item to the regression model is judged by evaluating the probability (P value) that the coefficient of each item is not zero. In this study, the acceptance probability for the coefficients was set at a P value less than 0.05 and the nonsignificant terms were eliminated, which did not impact the establishment and accuracy of the models. The regression models of slump flow (f_f), segregation rate (f_s), and bleeding rate (f_b) are shown in Table 5. The results of ANOVA are listed in Table 6. X_1 and X_2 are the coded values of slurry concentration and dosage of HPMC, respectively. Whether the model is effective depends on the following indicators. The first indicator is the P value of each model item; the P value less than 0.05 indicates that model terms are significant and the model has statistical significance. The second index is P value of lack of fit. When it is greater than 0.05, it indicates that the missing item of the model is not obvious, which means that it has nothing to do with pure error. The third index is the correlation coefficient (R^2) and the adjusted correlation coefficient (R_a^2) of the model; R^2 and R_a^2 varied between 0 and 1. If they presented high values (R^2 or $R_a^2 > 0.85$) that suggested a good correlation between the experimental results and the predicted values from models [29]. Observing the data in Table 6, it can be concluded that each index meets the requirements; the three regression models are effective and have good

Table 4: Test results.

Samples	Slump flow (mm)	Segregation rate (%)	Bleeding rate (%)
1#	850.00	26.00	3.90
2#	830.00	23.50	3.70
3#	650.00	18.56	0.00
4#	650.00	19.37	0.20
5#	642.00	9.47	1.11
6#	753.00	18.70	5.36
7#	740.00	17.50	5.25
8#	465.00	1.60	0.00
9#	518.00	4.16	1.23
10#	555.00	6.22	2.16
11#	385.00	0.40	0.27
12#	380.00	1.20	0.85
13#	400.00	3.10	1.80
14#	412.00	2.80	2.00
15#	320.00	0.00	0.00
16#	320.00	0.00	0.00

Table 5: Regression models.

Slump flow (mm)	$f_f = 546.9 - 210.78x_1 - 88.84x_2 + 46.29x_1x_2 + 28.56x_1^2$
Segregation rate (%)	$f_s = 4.38 - 6.32x_1 - 4.46x_2 + 2.69x_1x_2 + 6.38x_1^2 + 2.85x_2^2 - 5.5x_1^3$
Bleeding rate (%)	$f_b = 1.43 - 1.15x_1 - 2.08x_2 + 1.14x_1x_2 + 0.69x_2^2$

prediction ability. The corresponding relationship between the predicted value and the actual value is shown in Figure 5. It can be seen from the figure that the data points are basically distributed in a straight line. Therefore, the model can be used to analyze and predict the performance of CGFB slurry.

3.2. Performance Analysis of Fresh CGFB Slurry. In this work, the established regression models were used to illustrate the influence of various experimental factors and their binary interactions on CGFB properties in the modeled region. The detailed discussion of different properties of CGFB slurry is as follows.

3.2.1. Segregation Rate. The effect of slurry concentration and dosage of HPMC on segregation is shown in Figure 6. For the best visualization of results, the responses are clearly presented in two-dimensional contour map and three-dimensional plots. It can be seen from the figure that when the dosage of HPMC is fixed, with the increase of slurry concentration, the segregation rate of slurry will gradually decrease and eventually tend to 0, and the decrease rate of segregation rate from fast to slow. When the slurry concentration is fixed, with the increase of the content of HPMC, the change of segregation rate under different concentration is different. For example, when the concentration of slurry is 77%, the segregation rate of slurry will decrease from 30% to 21%, if the HPMC content is increased from 0% to 1%, and with the continuous increase of HPMC content, the segregation rate will gradually decrease and stabilize at about 19%. When the slurry concentration is 78%, with the increase of HPMC content, the segregation rate of slurry gradually decreases from 15% to 5%, when the slurry concentration is greater than 78.2%, with the increase of the content of HPMC, the segregation rate will be reduced to less than 5%. When the slurry concentration is greater than 79.7%, with the increase of the content of HPMC, the segregation rate of slurry will be reduced to 0%. Therefore, when the slurry concentration is too low (77%), the segregation can only be improved by increasing the slurry concentration. When the slurry concentration reaches a certain value (about 78.5%), the segregation rate can be reduced by adding HPMC or increasing the slurry concentration; the effect of the two methods is similar.

3.2.2. Slump Flow. Figure 7 shows the influence of slurry concentration and HPMC content on slump flow. It can be seen from the figure that the values of slump flow were most sensitive to the change of the slurry concentration, which can also be seen from the coefficient of slump flow regression equation. The coefficient of slurry concentration is −210.78, and the coefficient of HPMC content is −88.84. The negative influence of concentration on slump flow is three times of HPMC. With the increase of slurry concentration, the fluidity of slurry will be rapidly lost. In Section 3.2.1, the influence of slurry concentration and HPMC content on the segregation rate has been analyzed; combined with the characteristics that the slurry fluidity is more sensitive to the change of concentration, it is not difficult to find out that when the slurry concentration is low, the slurry segregation should be improved by increasing the concentration; when the concentration is increased to a certain value, the

Table 6: The results of ANOVA.

Source	Sum of squares	df	Mean square	F value	P value Prob > F	
Slump flow						
Model	$4.848E+005$	4	$1.212E+005$	1606.88	<0.0001	Significant
X_1	$4.393E+005$	1	$4.393E+005$	5824.86	<0.0001	
X_2	73673.23	1	73673.23	976.81	<0.0001	
X_1X_2	13427.18	1	13427.18	178.03	<0.0001	
X_1^2	2023.20	1	2023.20	26.82	0.0003	
Residual	829.65	11	75.42			
Lack of fit	473.15	6	78.86	1.11	0.4658	Not significant
Pure error	356.50	5	71.30			
Cor total	$4.856E+005$	15				
	R-squared		0.9983		Std. Dev.	8.68
Fit statistics	Adj R-squared		0.9977		C.V. %	1.57
	Pred R-squared		0.9965		Adeq precision	105.340
Segregation rate						
Model	1302.94	6	217.16	148.47	<0.0001	Significant
X_1	14.91	1	14.91	10.19	0.0110	
X_2	156.53	1	156.53	107.02	<0.0001	
X_1X_2	40.07	1	40.07	27.40	0.0005	
X_1^2	98.74	1	98.74	67.51	<0.0001	
X_2^2	17.11	1	17.11	11.70	0.0076	
X_1^3	9.31	1	9.31	6.36	0.0326	
Residual	13.16	9	1.46			
Lack of fit	8.95	4	2.24	2.65	0.1569	Not significant
Pure error	4.22	5	0.84			
Cor total	1316.10	15				
	R-squared		0.9900		Std. Dev.	1.21
Fit statistics	Adj. R-squared		0.9833		C.V. %	12.68
	Pred. R-squared		0.9631		Adeq precision	31.765
Bleeding rate						
Model	51.92	4	12.98	404.37	<0.0001	Significant
$X1$	13.19	1	13.19	410.82	<0.0001	
$X2$	41.18	1	41.18	1283.00	<0.0001	
$X1x2$	8.39	1	8.39	261.36	<0.0001	
$X22$	1.34	1	1.34	41.79	<0.0001	
Residual	0.35	11	0.032			
Lack of fit	0.29	6	0.048	3.62	0.0897	Not significant
Pure error	0.066	5	0.013			
Cor total	52.27	15				
	R-squared		0.9932		Std. Dev.	0.18
Fit statistics	Adj. R-squared		0.9908		C.V. %	10.30
	Pred. R-squared		0.9883		Adeq precision	51.719

segregation should be improved by adding suspending agent, which can both effectively improve the segregation of slurry and ensure the fluidity of slurry to the greatest extent.

3.2.3. Bleeding Rate. Figure 8 shows the influence of slurry concentration and dosage of HPMC on the bleeding rate. It can be seen from Figure 8 that compared with the concentration, HPMC has a greater impact on the bleeding rate of slurry. When the slurry concentration is constant, as long as the content of HPMC reaches 1.5%, the bleeding rate of slurry is basically reduced to 0%; however, when the content of HPMC is constant, the bleeding rate decreases slowly with the increase of slurry concentration, which is closely related to the hydroxyl groups with strong water absorption capacity in HPMC.

Generally, the smaller the bleeding rate is, the smaller the segregation rate is. However, by comparing the bleeding rate and segregation rate of slurry with 77% concentration, it can be found that the segregation rate cannot be characterized by the size of bleeding rate. When the content of HPMC is 1.5%, the bleeding rate of slurry has reached 0%, while the segregation rate of slurry is still as high as 19%. The reason may be that although HPMC adsorbs water to fine-grained materials (cement and fly ash), coarse aggregate gangue and fine-grained material still separate and gangue still sinks.

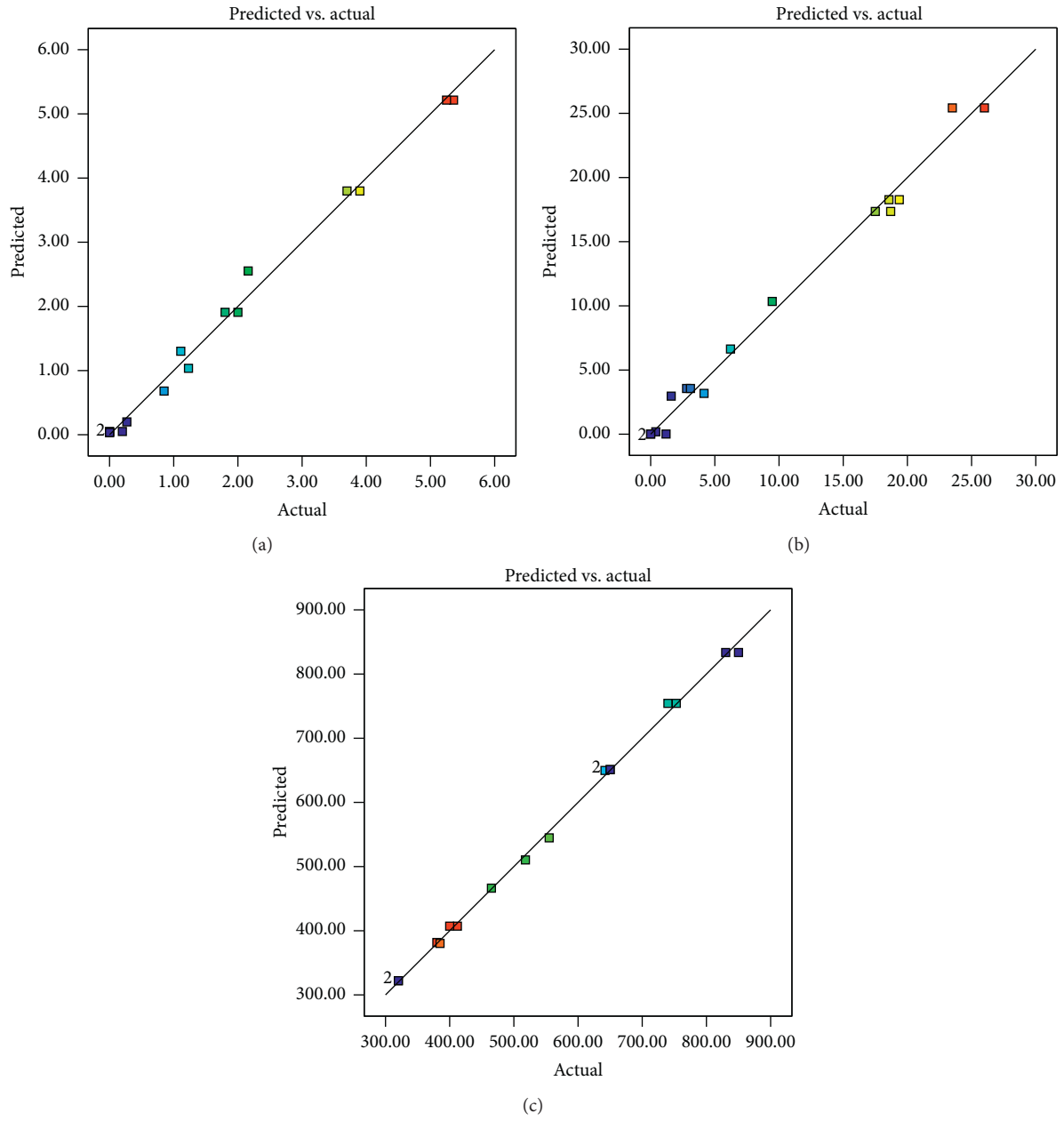

Figure 5: The corresponding relationship between predicted value and actual value. (a) Bleeding rate. (b) Segregation rate. (c) Slump flow.

4. Multiobjective Optimization and Model Verification

4.1. Multiobjective Optimization Based on Regression Model. The influence of slurry concentration and HPMC content on slurry segregation rate, slump expansion, and bleeding rate was analyzed. It was concluded that slurry concentration and HPMC content must have a proper ratio to ensure the performance of slurry meets the requirements, but there is no specific mix ratio range. Therefore, this section will use the established regression model to obtain the appropriate proportion range of slurry concentration and dosage of HPMC according to the working performance requirements of fresh slurry, so as to make CGFB slurry meets the requirements of each performance index as much as possible, without excessive damage to any other requirements. First of all, the specific criteria for the design of appropriate proportioning parameters are proposed. According to the field test, when the slump flow is more than 450 mm, the bleeding rate is less than 3%, and the segregation rate is less than 5%; the slurry can fill into the goaf smoothly through the pipeline and ensure that the underground working face is not affected by the bleeding of the slurry in the goaf. In the optimization module of Design-Expert 8.0.5 software, input the specific criterion requirements; the matching range meeting the requirements will be obtained, as shown in Figure 9. The satisfaction value of the red area in the figure is 1, which indicates that the slurry performance can meet the

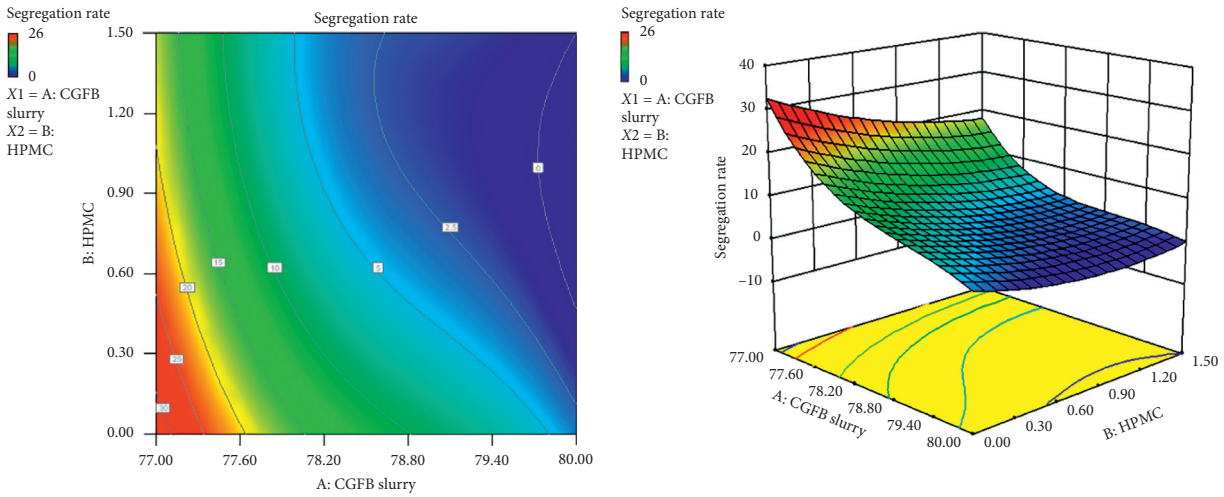

Figure 6: Response surface plot of segregation. (a) Two-dimensional diagram. (b) Three-dimensional diagram.

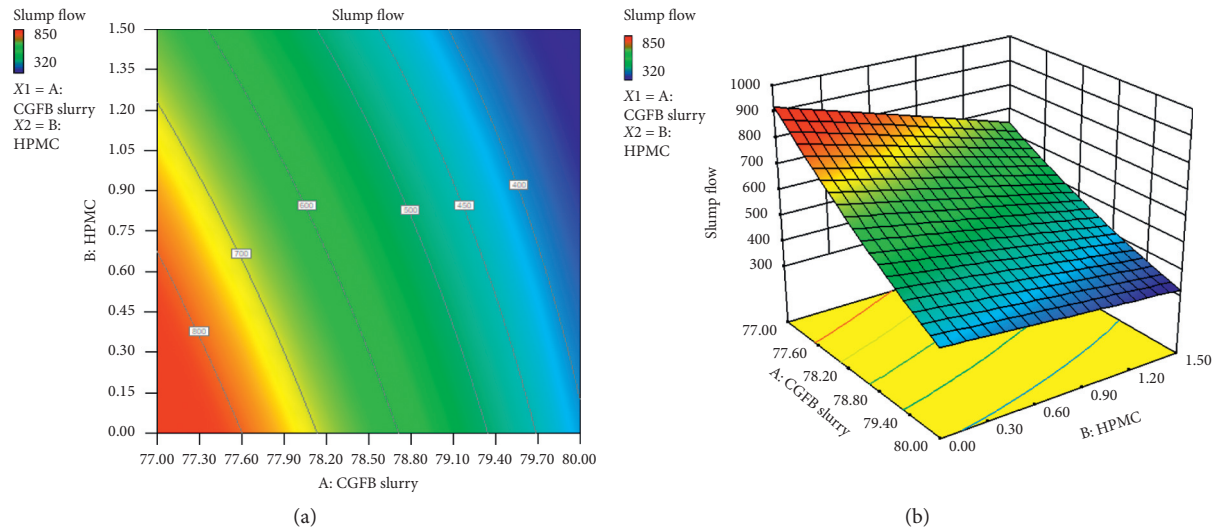

Figure 7: Response surface plot of slump flow. (a) Two-dimensional diagram. (b) Three-dimensional diagram.

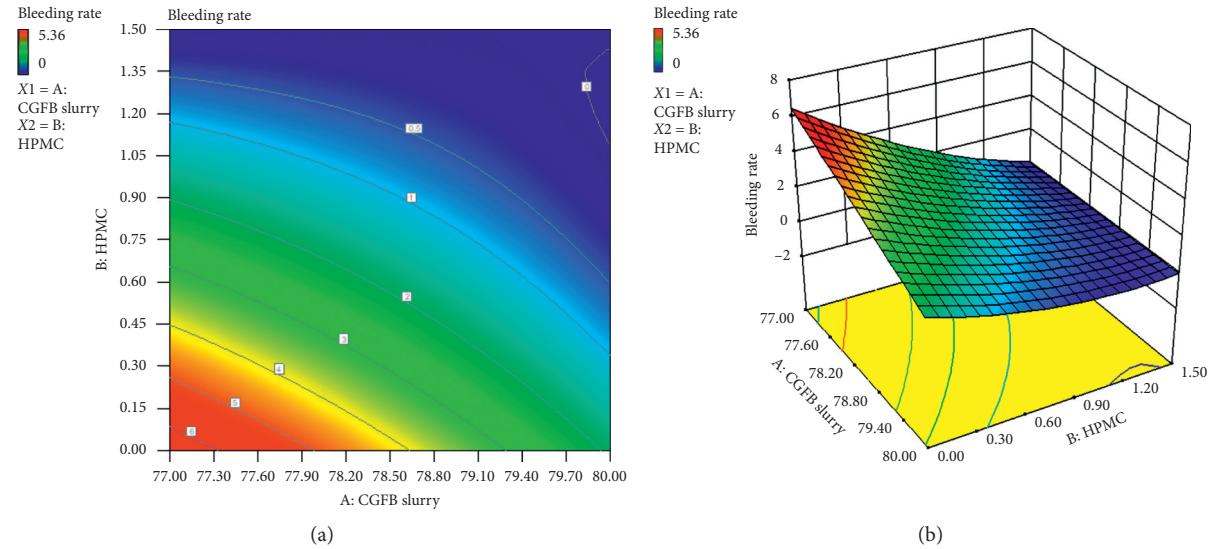

Figure 8: Response surface plot of bleeding rate. (a) Two-dimensional diagram. (b) Three-dimensional diagram.

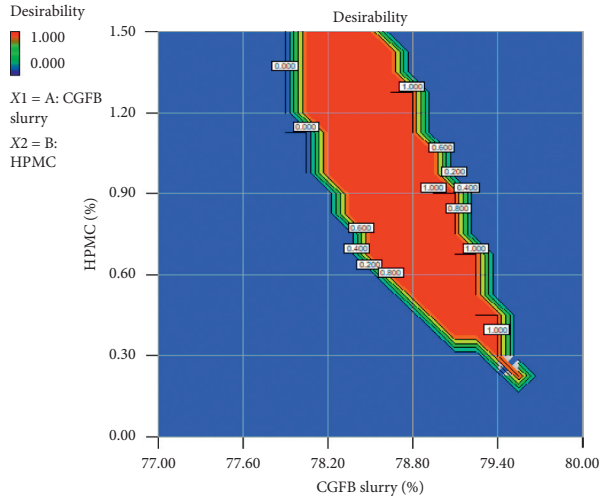

Figure 9: Multiobjective optimization results.

Table 7: Material proportioning scheme of the three samples.

Samples	Solids content (wt. %)	Cement content (wt. %)	Fly ash content (wt. %)	Coal gangue content (wt. %)	HPMC content/powder (wt. %)	Water content (wt. %)
S1	78.50	12	19.00	47.50	1.0	21.50
S2	78.80	12	19.09	47.71	0.7	21.20
S3	79.00	12	19.14	47.86	0.5	21.00

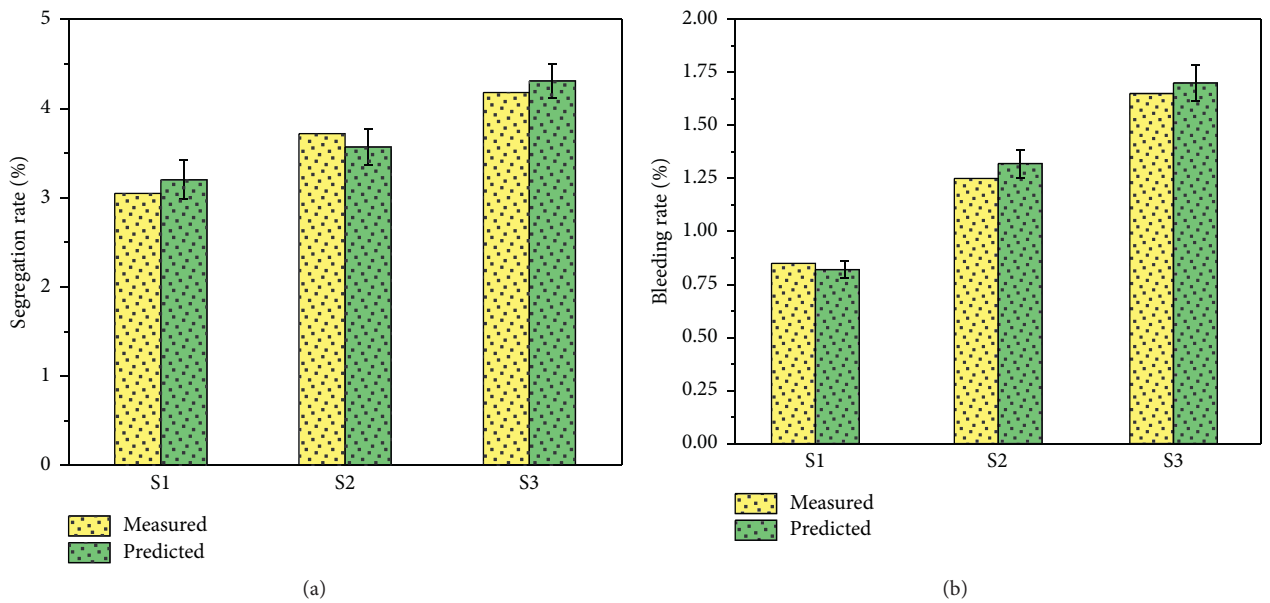

Figure 10: Continued.

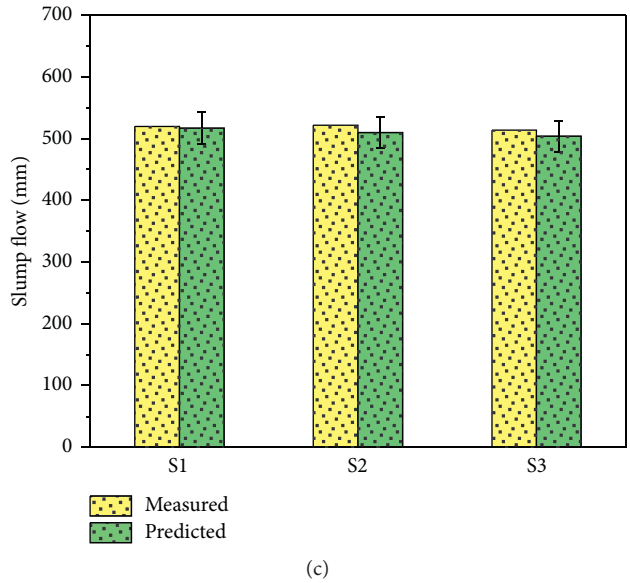

(c)

Figure 10: The comparison between the predicted values and the measured values. (a) Segregation rate. (b) Bleeding rate. (c) Slump flow.

requirements when the mixture ratio of slurry concentration and HPMC content is within this range. The satisfaction of the blue area is 0, which means that the mix ratio of slurry concentration and HPMC content cannot meet the requirements of slurry performance. What needs to be explained here is that in the research of this paper, although the mix proportion in the red area can meet the requirements, due to the high price of HPMC, high HPMC content will affect the cost of filling mining, so the proportion with less suspension agent should be adopted in the actual mix proportion.

4.2. Model Validation. In order to verify the effectiveness of the model, this paper selects three matching schemes which meet the requirements from the area with satisfaction of 1 and conducts additional tests; the schemes are shown in Table 7. Figure 10 gives a comparative view of the predicted values and measured values for the tested mixtures. In this figure, one can observe that all measured values fall within the limits of the prediction intervals corresponding to a 95% confidence level. Thus, it was revealed that there was a good agreement between the experimental results and predicted results from the statistical models.

5. Conclusion

Based on response surface methodology, the effects of concentration and HPMC on slump flow, segregation rate, and bleeding rate of CGFB slurry were studied. The main conclusions are as follows:

(1) According to the test results of 16 groups of tests, the regression models of slump flow, segregation rate, and bleeding rate of slurry are established, and the validity and accuracy of the models are analyzed. The results show that the established models are effective, and all models have the ability to predict the performance characteristics of CGFB slurry.

(2) According to the three regression models, the slurry performance is analyzed; it is concluded that the segregation rate and slump flow of slurry are more sensitive to the change of concentration, and the bleeding rate of slurry is more sensitive to the change of HPMC content.

(3) When the slurry concentration is too low, the increase of HPMC content cannot effectively control the segregation of slurry; only by increasing the slurry concentration, the segregation of slurry can be improved. When the concentration is increased to a certain value, the segregation rate of slurry can be reduced by adding the appropriate amount of HPMC or continuously increasing the concentration of slurry. The effect of the two methods is similar.

(4) Based on the three regression models, according to the performance requirements of slurry, the mixture ratio range of slurry concentration and HPMC content is obtained. In addition, three new CGFB mixtures have been tested, and the experimental results are in good agreement with the predicted values.

Data Availability

The datasets used or analyzed during the current study are available from the corresponding author upon reasonable request.

Conflicts of Interest

The authors declare that they have no conflicts of interest regarding the publication of this paper.

References

[1] G. Zhang, L. Chen, Z. Wen et al., "Squeezing failure behavior of roof-coal masses in a gob-side entry driven under unstable overlying strata," *Energy Science & Engineering*, vol. 8, no. 7, pp. 2443–2456, 2020.

[2] F. G. Bell, T. R. Stacey, and D. D. Genske, "Mining subsidence and its effect on the environment: some differing examples," *Environmental Geology*, vol. 40, no. 1-2, pp. 135–152, 2000.

[3] R. D. Lokhande, A. Prakash, K. B. Singh, and K. K. K. Singh, "Subsidence control measures in coalmines: a review," *Journal of Scientific and Industrial Research*, vol. 64, no. 5, pp. 323–332, 2005.

[4] S. Horiuchi, M. Kawaguchi, and K. Yasuhara, "Effective use of fly ash slurry as fill material," *Journal of Hazardous Materials*, vol. 76, no. 2-3SI, pp. 301–337, 2000.

[5] G.-C. Zhang, Y. Tan, S.-J. Liang, and H.-G. Jia, "Numerical estimation of suitable gob-side filling wall width in a highly gassy longwall mining panel," *International Journal of Geomechanics*, vol. 18, no. 8, 2018.

[6] B. Li, N. Zhou, W. Qi, A. Li, and Z. Cui, "Surface subsidence control during deep backfill coal mining: a case study," *Advances in Civil Engineering*, vol. 2020, Article ID 6876453, 2020.

[7] J.-F. Zha, G.-L. Guo, W.-K. Feng, and Q. Wang, "Mining subsidence control by solid backfilling under buildings," *Transactions of Nonferrous Metals Society of China*, vol. 21, pp. S670–S674, 2011.

[8] Q. Wu, J. Pang, S. Qi et al., "Impacts of coal mining subsidence on the surface landscape in Longkou city, Shandong Province of China," *Environmental Earth Sciences*, vol. 59, no. 4, pp. 783–791, 2009.

[9] G. C. Zhang, Z. J. Wen, S. J. Liang et al., "Ground response of a gob-side entry in a longwall panel extracting 17 m-thick coal seam: a case study," *Rock Mechanics and Rock Engineering*, vol. 53, no. 2, pp. 497–516, 2020.

[10] D. Wu, B. Yang, and Y. Liu, "Pressure drop in loop pipe flow of fresh cemented coal gangue-fly ash slurry: experiment and simulation," *Advanced Powder Technology*, vol. 26, no. 3, pp. 920–927, 2015.

[11] B. Yin, T. Kang, J. Kang, and Y. Chen, "Experimental and mechanistic research on enhancing the strength and deformation characteristics of fly-ash-cemented filling materials modified by electrochemical treatment," *Energy & Fuels*, vol. 32, no. 3, pp. 3614–3626, 2018.

[12] J. Hou, Z. Guo, W. Liu, and Y. Zhang, "Mechanical properties and meso-structure response of cemented gangue-fly ash backfill with cracks under seepage- stress coupling," *Construction and Building Materials*, vol. 250, Article ID 118863, 2020.

[13] M. Li, J. Zhang, A. Li, and N. Zhou, "Reutilisation of coal gangue and fly ash as underground backfill materials for surface subsidence control," *Journal of Cleaner Production*, vol. 254, Article ID 120113, 2020.

[14] Y. Wang, Y. Huang, and Y. Hao, "Experimental study and application of rheological properties of coal gangue-fly ash backfill slurry," *Processes*, vol. 8, no. 3, p. 284, 2020.

[15] D. Wu, B. Yang, and Y. Liu, "Transportability and pressure drop of fresh cemented coal gangue-fly ash backfill (CGFB) slurry in pipe loop," *Powder Technology*, vol. 284, pp. 218–224, 2015.

[16] X. Yang, B. Xiao, Q. Gao, and J. He, "Determining the pressure drop of cemented Gobi sand and tailings paste backfill in a pipe flow," *Construction and Building Materials*, vol. 255, Article ID 119371, 2020.

[17] X. Du, G. Feng, Y. Zhang, Z. Wang, Y. Guo, and T. Qi, "Bearing mechanism and stability monitoring of cemented gangue-fly ash backfill column with stirrups in partial backfill engineering," *Engineering Structures*, vol. 188, pp. 603–612, 2019.

[18] G. Feng, X. Du, and Y. Zhang, ""Optical-acoustic-stress" responses in failure progress of cemented gangue-fly ash backfill material under uniaxial compression," *Nondestructive Testing and Evaluation*, vol. 34, no. 2, pp. 135–146, 2019.

[19] Q. Li, G. Feng, Y. Guo et al., "The dosage of superplasticizer in cemented coal waste backfill material based on response surface methodology," *Advances in Materials Science and Engineering*, vol. 2019, Article ID 5328523, 8 pages, 2019.

[20] J. Yang, B. Yang, and M. Yu, "Pressure study on pipe transportation associated with cemented coal gangue fly-ash backfill slurry," *Applied Sciences*, vol. 9, no. 3, p. 512, 2019.

[21] D. Wu, T. Deng, and R. Zhao, "A coupled THMC modeling application of cemented coal gangue-fly ash backfill," *Construction and Building Materials*, vol. 158, pp. 326–336, 2018.

[22] D. Wu, Y. Hou, T. Deng, Y. Chen, and X. Zhao, "Thermal, hydraulic and mechanical performances of cemented coal gangue-fly ash backfill," *International Journal of Mineral Processing*, vol. 162, pp. 12–18, 2017.

[23] J. Yang, *Rheological Study on Cemented Coal Gangue Fly-Ash Backfill Slurry Associated with Fly Ash Impacts*, Trans Tech Publications Ltd, Incheon, Korea, 2020.

[24] J. Yang, B. Yang, T. Li, and M. Yu, "Fluidity study on chemical behavior of Bingham materials in pipe transportation," *Chemical Engineering Transactions*, vol. 71, pp. 1051–1056, 2018.

[25] L. Khare, T. Karve, R. Jain, and P. Dandekar, "Menthol based hydrophobic deep eutectic solvent for extraction and purification of ergosterol using response surface methodology," *Food Chemistry*, vol. 340, Article ID 127979, 2021.

[26] S. Pandey, A. Kumar, and P. S. Rao, "Optimization, modeling, and characterization study for the physicochemical properties of raw banana and defatted soy composite extrudates," *Food Chemistry*, vol. 339, Article ID 127865, 2021.

[27] M. Preskar, D. Videc, F. Vrečer, and M. Gašperlin, "Investigation of design space for freeze-drying injectable ibuprofen using response surface methodology," *Acta Pharmaceutica*, vol. 71, no. 1, pp. 81–98, 2021.

[28] C. Zhao, L. Wang, F. Zhang, and F. Yang, "A method to balance dynamic current of paralleled SiC MOSFETs with Kelvin connection based on response surface model and nonlinear optimization," *IEEE Transactions on Power Electronics*, vol. 36, no. 2, pp. 2068–2079, 2021.

[29] W. Yan, G. Wu, and Z. Dong, "Optimization of the mix proportion for desert sand concrete based on a statistical model," *Construction and Building Materials*, vol. 226, pp. 469–482, 2019.

[30] A. N. S. Alqadi, K. N. B. Mustapha, S. Naganathan, and Q. N. S. Al-Kadi, "Uses of central composite design and surface response to evaluate the influence of constituent materials on fresh and hardened properties of self-compacting concrete," *KSCE Journal of Civil Engineering*, vol. 16, no. 3, pp. 407–416, 2012.

[31] K. E. Alyamac, E. Ghafari, and R. Ince, "Development of eco-efficient self-compacting concrete with waste marble powder using the response surface method," *Journal of Cleaner Production*, vol. 144, pp. 192–202, 2017.

[32] C. Chen and K. Chiang, "Analyzing the design of vibration reduction with the rubber-layered laminates in the precision turning with a diamond cutting tool," *International Journal of Advanced Manufacturing Technology*, vol. 57, no. 1–4, pp. 101–116, 2011.